

A NEW FREQUENCY SELECTIVE WINDOW FOR CONSTRUCTING WAVEGUIDE BANDPASS FILTERS WITH MULTIPLE ATTENUATION POLES

M. Tsuji and H. Deguchi

Department of Electronics,
Doshisha University, Kyotanabe, Kyoto 610-0321, Japan

M. Ohira

Graduate School of Science and Engineering
Saitama University
Sakura-ku, Saitama City, Saitama 338-8570, Japan

Abstract—This paper presents a novel frequency selective window for waveguide filters. It has a resonant characteristic with two attenuation poles on both sides of a passband, that is, a dual-behavior resonance. Such frequency selective windows make it possible to construct a compact bandpass filter having multiple attenuation poles without any additional coupling structures. As design examples, we show 3-pole Chebyshev waveguide filters with six attenuation poles in both the microwave and the millimeter-wave regions. The validity of the present filters is proven by the comparison of the frequency characteristics between the calculated and the measured results.

1. INTRODUCTION

Recently microwave and millimeter-wave waveguide filters with higher performance and more compact are required [1–3]. To design a bandpass filter with multiple attenuation poles (transmission zeros), the dual-behavior resonator [4, 5] is one of the attractive resonators. The dual-behavior resonator provides one resonance (full transmission) in a passband and two anti-resonances (full reflection) in stopbands at both sides of the passband, while conventional resonators provide one resonance for constructing a specified passband [6, 7]. To utilize high

flexibility of the dual-behavior resonators in rectangular-waveguide filters, we have already proposed a novel resonator called a frequency-selective surface (FSS) [8–11]. The FSS consists of thin conductor supported by a dielectric substrate, and its dual-behavior resonance is realized by the combination of the aperture-type and the patch-type FSSs. Our proposed FSS is more suitable for obtaining a sharp-skirt response than previous ones [12,13]. However, the dielectric substrate of FSS-loaded waveguide filters brings the insertion loss in the passband due to dielectric loss and also makes installation and mechanical stability difficult. Therefore, if developing a new window resonator without a dielectric support instead of the conventional FSSs, it will be very useful in practice.

In this paper, we propose a new window resonator constructed by only a conductor, which has also both aperture-type and patch-type behaviors like previously developed FSS resonators. We call hereafter the metallic thin resonator a frequency selective window, since the proposed resonator has the additional function providing attenuation poles unlike conventional resonant irises. To design a waveguide filter using the frequency selective window, its resonant characteristic is first investigated for various structural parameters. As a design example, we demonstrate third-order bandpass filters having six attenuation poles at the both sides of the passband, of which the bandwidth is 4% at the center frequency 10 GHz [14]. Although the effect of the window thickness on filter characteristics was not clear in the previous discussion [14], we clarify here this point and redesign windows by taking their thickness into account. Furthermore, we apply the proposed windows to a waveguide filter in the millimeter-wave region. The measurements of the transmission characteristics for the fabricated filters in both frequency regions are also performed and compared with the calculated results.

2. FREQUENCY SELECTIVE WINDOW

2.1. Filter Structure

Figures 1(a) and (b) show the overall structure of the waveguide filter constructed by the proposed resonators (frequency selective windows), and the geometrical parameters of the window, respectively. The section size of the rectangular waveguide is $a \times b$. The frequency selective windows are located at the interval of the length l . The length l can be chosen arbitrarily [8,9]. For simplicity, l is set here to be a quarter wavelength, so that the waveguide between the frequency selective windows works as an ideal inverter. In the design, the conductor of the frequency selective windows is assumed to be

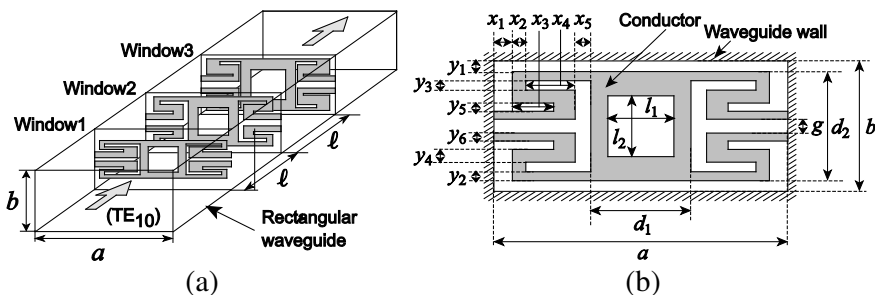


Figure 1. Waveguide filter made of frequency selective windows. (a) Overall structure and (b) geometrical parameters of the frequency selective window.

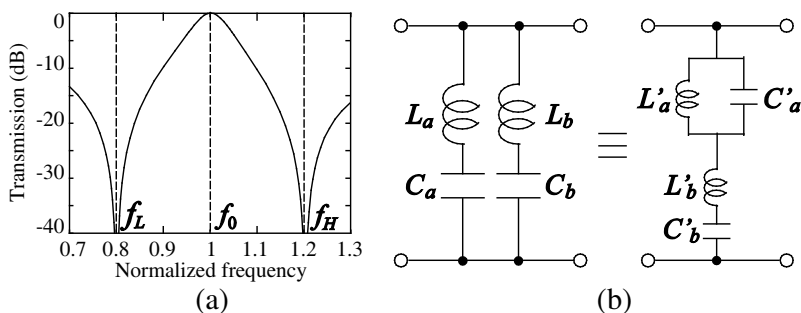


Figure 2. (a) An example of transmission response of a frequency selective window and (b) its equivalent circuit.

infinitesimally thin. The shape of the frequency selective window in Fig. 1(b) is obtained by modifying the element shape of the four-armed square loop FSS [10] proposed by us. The window is symmetrical with respect to the vertical and the horizontal axes of the waveguide, and is composed of a square loop ($d_1 \times d_2$) having an inner aperture ($l_1 \times l_2$) and four arms ($x_i, i = 1, 2, \dots, 5, y_j, j = 1, 2, \dots, 6$) folded like a meander line. The ends of these arms are connected to the waveguide side walls, so that any dielectric support is not required.

2.2. Equivalent Circuit

The present window resonator has the resonant frequency f_0 (full transmission) for constructing a passband and two anti-resonant frequencies f_L and f_H (full reflection, $f_L < f_0 < f_H$) for providing attenuation poles, as shown in Fig. 2(a). Such a transmission response can be easily expressed by either of two equivalent circuit models shown

in Fig. 2(b) corresponding to resonant or anti-resonant characteristics. Two series resonant circuits L_a, C_a and L_b, C_b produce two anti-resonant characteristics at the frequencies f_L and f_H . On the other hand, the parallel resonant circuit L'_a, C'_a resonates at the center frequency f_0 , and then the series resonant circuits L'_b, C'_b is in the off-resonance. Then the parallel resonant-circuit parameters L'_a and C'_a which have an important role to produce a passband are related with the circuit parameters L_a, C_a, L_b and C_b by the following equations.

$$C_a = (L'_a/4\pi^2 - f_H^2 C'_a)/(f_L^2 - f_H^2), \quad L_a = 1/(4\pi^2 f_L^2 C_a) \quad (1)$$

$$C_b = (L'_a/4\pi^2 - f_L^2 C'_a)/(f_H^2 - f_L^2), \quad L_b = 1/(4\pi^2 f_H^2 C_b) \quad (2)$$

2.3. Resonant Mechanism

To obtain a response shown in Fig. 2(a), the frequency selective window utilizes the resonance of both electric and the magnetic currents. To understand the resonant mechanism, Fig. 3 depicts rough sketches of the electric and the magnetic current paths at the resonant and anti-resonant frequencies. At the resonant frequency f_0 , the magnetic currents flow on the aperture (that is, non-metal part) except for the central aperture ($l_1 \times l_2$) as shown in Fig. 3(a). Then, the window works as an aperture type resonator that provides full transmission. On the other hand, we can see from Figs. 3(b) and (c) that the window has different current paths on the conductor at two anti-resonant frequencies f_L and f_H . At the first anti-resonance, the electric currents flow on the path A ($\lambda_g/4$, λ_g : wavelength in a waveguide) and the path B ($\lambda_g/2$), while at the second anti-resonance they flow on the path C at the corners of four arms. At these anti-resonant frequencies, the window works as a patch-type resonator that provides full reflection. As a result, the proposed frequency selective window successfully behaves as both aperture-type and patch-type resonators in a narrow frequency band.

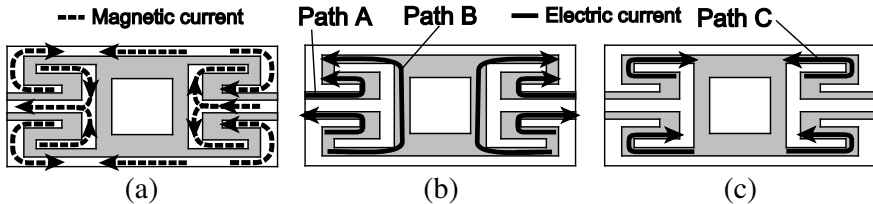


Figure 3. (a) Magnetic current distribution at resonant frequency f_0 , (b) electric current distributions at the first anti-resonance f_L and (c) at the second anti-resonance f_H .

3. RESONANT CHARACTERISTICS

The frequency responses of the frequency selective window are calculated by the HFSS. We investigate numerically the dependence of the geometrical parameters for the proposed resonator in the X-band region, in order to control the resonant frequencies f_0 , f_L and f_H . Fig. 4 shows the transmission responses of the frequency selective windows. Although the frequency selective window in Fig. 1(b) has many geometrical parameters, the responses for three parameters x_3 , x_4 and l_1 that are sensitive for the resonant and anti-resonant frequencies are shown here.

It can be seen from Fig. 4(a) that as increasing the length x_3 (the length $x_2 + x_4$ is kept constant), the first anti-resonant frequency f_L shifts to lower frequency side drastically, compared with the second

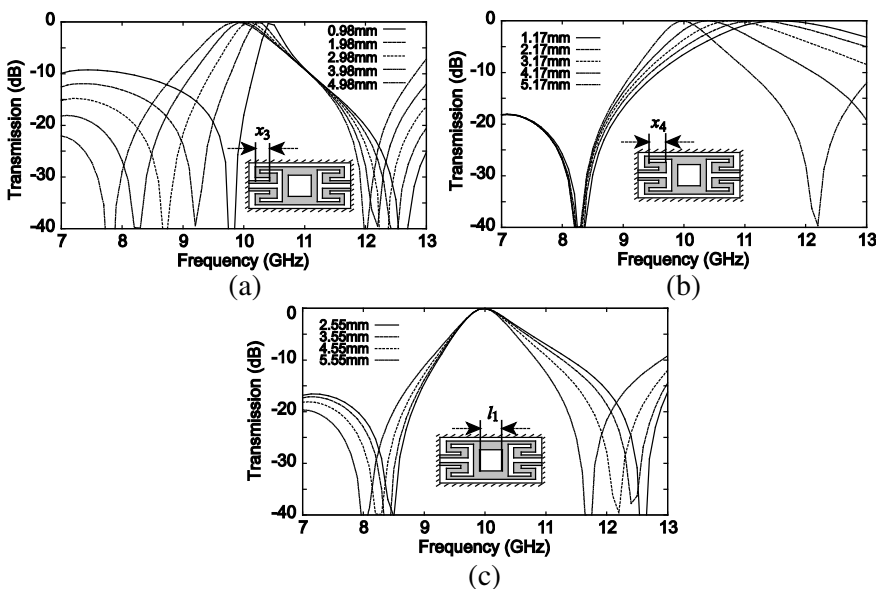


Figure 4. Transmission characteristics of the proposed metallic window for various lengths of (a) x_3 (fixed parameters: $x_2 = 0.81$ mm, $x_4 = 5.17$ mm, $l_1 = 4.55$ mm), (b) x_4 (fixed parameters: $x_3 = 3.98$ mm, $l_1 = 4.55$ mm), and (c) l_1 (fixed parameters: $x_2 = 0.81$ mm, $x_3 = 3.98$ mm, $x_4 = 5.17$ mm). Common parameters: $x_1 = 0.31$ mm, $x_5 = 1.00$ mm, $y_1 = 0.31$ mm, $y_2 = 0.78$ mm, $y_3 = 0.50$ mm, $y_4 = 1.49$ mm, $y_5 = 0.50$ mm, $y_6 = 1.01$ mm, $g = 0.99$ mm, $d_1 = 8.29$ mm, $d_2 = 9.54$ mm, $l_2 = 4.98$ mm. Waveguide size: $a \times b = 22.86 \times 10.16$ mm².

one f_H and the resonant frequency f_0 . So, the length x_3 determines mainly the anti-resonant frequency f_L . The reason is that the length of the current path A in Fig. 3(b) depends on the length x_3 . On the other hand, the length of the current path C in Fig. 3(c) is mainly decided by the length x_4 . Thus, the second anti-resonant frequency f_H can be controlled by adjusting the length x_4 as shown in Fig. 4(b). Then the first one f_L is almost not affected by the change of x_4 (the length $(x_2 + x_4)$ is kept constant), since the length x_3 for the path A and the length $x_2 + x_4$ for the path B are not changed.

Furthermore, increasing the length l_1 makes f_L and f_H shift to lower frequency side simultaneously, keeping the resonant frequency f_0 as shown in Fig. 4(c). This effect can be explained by no flow of the magnetic current in the central aperture ($l_1 \times l_2$) as shown in Fig. 3(a) can explain this effect. As demonstrated here, the interval of three resonant frequencies f_0 , f_L and f_H can be controlled by adjusting the lengths x_3 , x_4 and l_1 . Consequently, by combining the frequency selective windows with the same center frequency, but with the different anti-resonant frequencies, we can construct a high-performance bandpass filter with multiple attenuation poles without any additional coupling structures.

4. DESIGN EXAMPLE AND EXPERIMENTS

4.1. Design Procedure

We now show a design example of the third-order waveguide filter using the proposed frequency selective windows. The filter can be expressed as the equivalent filter network shown in Fig. 5. The admittance inverters (J inverters) connected to the input/output waveguides have $J_{01} = J_{34} = 1$ and those between the FSSs have also $J_{12} = J_{23} = 1$ since the length of the waveguide section is chosen to be $\lambda_g/4$. Then the relation between the J inverter and the circuit parameters L'_{ai} and C'_{ai}

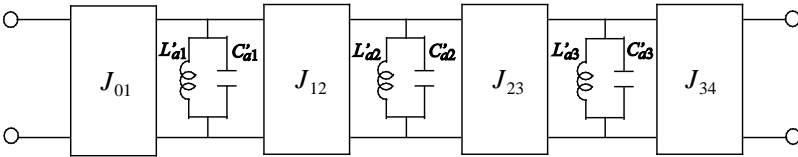


Figure 5. Equivalent circuit expression using admittance inverters (J inverters) to design a passband.

($i = 1, 2, 3$) are given by the following equations [15].

$$\begin{aligned}
 J_{01} &= (2\pi f_0 w C'_{a1} G_0 / g_1)^{1/2}, & J_{12} &= (2\pi f_0 w) \{C'_{a1} C'_{a2} / (g_1 g_2)\}^{1/2} \\
 J_{23} &= (2\pi f_0 w) \{C'_{a2} C'_{a3} / (g_2 g_3)\}^{1/2}, & J_{34} &= (2\pi f_0 w C'_{a3} G_4 / g_3)^{1/2} \\
 L'_{ai} &= 1 / (4\pi^2 f_0^2 C'_{ai}) \quad (i = 1, 2, 3),
 \end{aligned} \tag{3}$$

where w is the ratio of the bandwidth and g_i is the coefficient determined by a bandpass property. Therefore, when such a property is specified, the circuit parameters L'_{ai} and C'_{ai} are determined by Eq. (3). Then, the equivalent circuit parameters L_{ai} , C_{ai} , L_{bi} and C_{bi} ($i = 1, 2, 3$) shown in Fig. 2 are calculated from Eqs. (1) and (2), and an ideal resonant curve of each frequency selective window is obtained. Finally, the geometrical parameters shown in Fig. 1(b) are determined so that the resonant characteristic of each frequency selective window can be fitted to the ideal one in both the passband and stopband regions.

4.2. Design of Microwave Filter and Experiment

As an example, the passband response is approximated by 3-pole 0.01 dB Chebyshev at the center frequency $f_0 = 10$ GHz and the frequency bandwidth $f_w = 400$ MHz. In the stopbands, the filter is designed to have six attenuation poles as follows:

$$\begin{aligned}
 \text{Window 1: } & f_{L1} = 9 \text{ GHz}, & f_{H1} &= 11 \text{ GHz} \\
 \text{Window 2: } & f_{L2} = 8 \text{ GHz}, & f_{H2} &= 12 \text{ GHz} \\
 \text{Window 3: } & f_{L3} = 7 \text{ GHz}, & f_{H3} &= 13 \text{ GHz}
 \end{aligned}$$

The main rectangular waveguide is a WR-90 ($a = 22.86$ mm, $b = 10.16$ mm). Table 1 gives dimension of the designed frequency selective

Table 1. Dimension of the frequency selective windows in the microwave region.

	Window 1	Window 2	Window 3		Window 1	Window 2	Window 3
x_1	0.32 mm	0.53 mm	0.48 mm	y_4	0.42 mm	1.73 mm	2.81 mm
x_2	0.85 mm	1.15 mm	2.81 mm	y_5	0.42 mm	0.36 mm	4.95 mm
x_3	4.05 mm	3.54 mm	4.95 mm	y_6	0.96 mm	0.96 mm	3.14 mm
x_4	5.93 mm	4.74 mm	3.14 mm	g	0.56 mm	1.08 mm	0.33 mm
x_5	0.49 mm	0.95 mm	0.33 mm	d_1	7.68 mm	8.12 mm	0.20 mm
y_1	1.93 mm	0.25 mm	0.20 mm	d_2	6.31 mm	9.66 mm	0.48 mm
y_2	0.57 mm	0.65 mm	0.48 mm	l_1	7.00 mm	5.35 mm	0.53 mm
y_3	0.50 mm	0.59 mm	0.53 mm	l_2	5.47 mm	7.96 mm	2.08 mm

windows. Fig. 6 shows the comparison of transmission responses of each frequency selective window between the calculated results and the ideal curves by the *LC* prototype equivalent circuit. As clearly seen from the characteristic of the window 3 in Fig. 6(c), it is difficult to set the attenuation pole at the frequency positions far from the center frequency. Fig. 7 shows the insertion and the return losses of the bandpass filter constructed by setting these three frequency selective windows at the interval of $\lambda_{g0}/4$. The filter structure is shown in the inset of the figure and the filter characteristics with windows of 0 mm

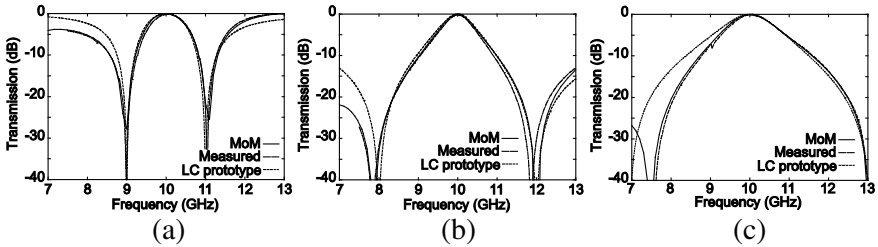


Figure 6. Comparison of transmission characteristic between the calculated results of the designed windows of 0 mm in thickness and the equivalent circuit approach. (a) Window 1, (b) window 2 and (c) window 3.

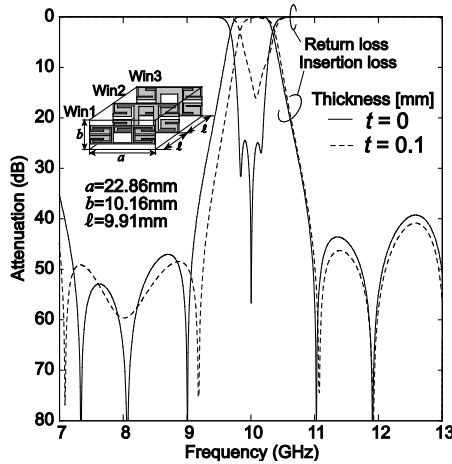


Figure 7. Calculated frequency characteristics of insertion and return losses for the designed filter. The solid lines show the results for the windows with zero-thickness and the dashed lines are for the windows with 0.1 mm-thickness.

in thickness are indicated by the solid lines. In the simulation, the conductor loss is not taken into account. The filter obtained by our design method provides the specified passband and the six attenuation poles at the stopbands successfully. The total longitudinal length of the filter is just $\lambda_{g0}/2$. To compare with the experimental results, Fig. 7 also shows the filter characteristics calculated by considering the thickness ($t = 0.1$ mm) of the windows that is used in experiments. These are indicated by the dashed lines. We can observe that the filter characteristics are deteriorated by the effect of the thickness in both the passband and stopband.

So we again design the windows of 0.1 mm in thickness by adjusting three lengths x_3 , x_4 , and l_1 (the length $x_2 + x_4$ is kept constant) in the structural parameters shown in Table 1. Fig. 8 shows the photographs of the fabricated windows with the surrounding metallic frame that are newly designed by considering the thickness of the windows. Their calculated and measured frequency characteristics are given in Fig. 9. It can be confirmed from excellent agreement between the measured and the calculated results that each of fabricated windows works well as a dual-behavior resonator having the specified resonant and anti-resonant frequencies. Fig. 10 shows the insertion and the return losses of the bandpass filter constructed by using these three windows, where the dotted lines indicate the measured results and the solid lines are the calculated ones. In the calculation, the conductor loss ($\sigma = 5.8 \times 10^8$ S/m) of the copper is taken into account. Agreement between both results is very good over the whole frequency. The insertion loss at the center frequency in the measurement is 0.58 dB,

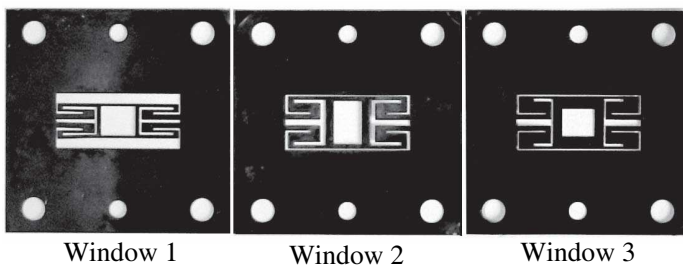


Figure 8. Photograph of the fabricated windows that are newly designed by considering their thickness of 0.1 mm. The lengths x_3 , x_4 , and l_1 (the length $x_2 + x_4$ is kept constant) in the structural dimensions shown in Fig. 5 are adjusted as follows: Window 1: $x_3 = 4.71$ mm, $x_4 = 5.89$ mm, $l_1 = 6.40$ mm. Window 2: $x_3 = 4.44$ mm, $x_4 = 4.84$ mm, $l_1 = 4.95$ mm. Window 3: $x_3 = 5.55$ mm, $x_4 = 3.34$ mm, $l_1 = 5.53$ mm.

while that in the calculation is 0.38 dB.

Finally, Fig. 11 compares the group delay of the filter between the calculated and the measured results. Both results agree well with each other and show to have a relatively flat group-delay response within the passband.

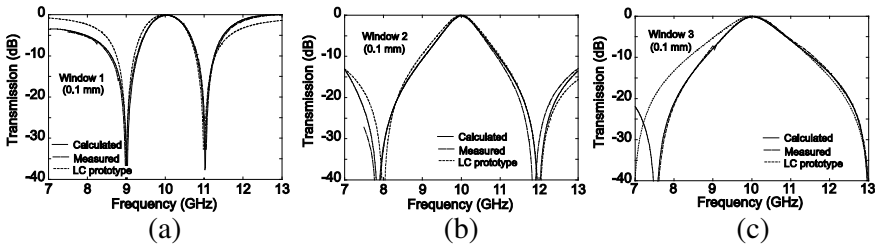


Figure 9. Comparison of transmission characteristic between the calculated results of the designed windows of 0.1 mm in thickness and the measured ones. (a) Window 1, (b) window 2 and (c) window 3.

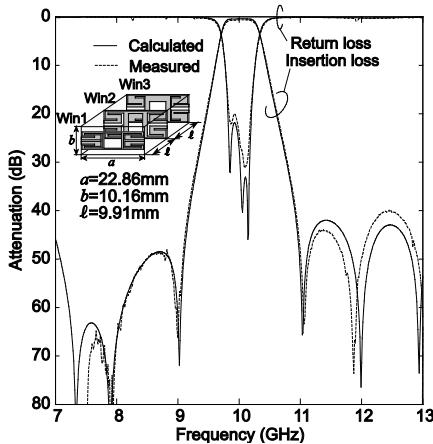


Figure 10. Comparison of insertion and return losses of the designed filter with the 0.1 mm-thick windows between the calculated and the measured results. In the calculation, the conductor loss ($\sigma = 5.8 \times 10^8$ S/m) of the copper is taken into account.

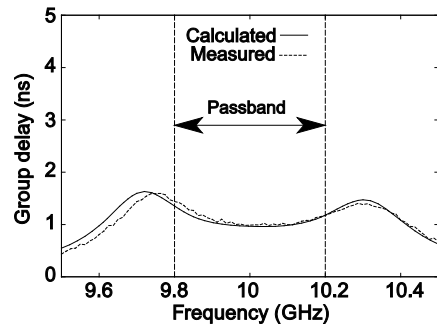


Figure 11. Comparison of group delay of the designed filter between the calculated and the measured results.

4.3. Design of Millimeter-wave Filter and Experiment

As an example, the millimeter-wave filter is designed here at the center frequency $f_0 = 50$ GHz and the frequency bandwidth $f_w = 2$ GHz. This filter has the same Chebyshev response with the previous examples in the passband and six attenuation poles at the following frequencies in the stopbands.

$$\text{Window 1: } f_{L1} = 45 \text{ GHz, } f_{H1} = 55 \text{ GHz}$$

$$\text{Window 2: } f_{L2} = 40 \text{ GHz, } f_{H2} = 60 \text{ GHz}$$

$$\text{Window 3: } f_{L3} = 35 \text{ GHz, } f_{H3} = 65 \text{ GHz}$$

The main rectangular waveguide is a WR-17 ($a = 4.78$ mm, $b = 2.39$ mm). We now recognize the effect of the thickness of the frequency selective windows on the transmission characteristics from the example in the previous section. So in the design calculation, we take the window's thickness of 0.04 mm into account. The dimension of the windows obtained by the design is given in Table 2. Fig. 12 shows comparison of the transmission responses of each window between the calculated results and the ideal curves by the LC prototype equivalent circuit. As expected from Fig. 6, the characteristic of the window 3 does not perfectly fit with that of the ideal curve. Fig. 13 shows the insertion and the return losses of the bandpass filter constructed by setting these frequency selective windows at the interval of $\lambda_{g0}/4$, where the conductor loss is not taken into account. We can observe the filter is successfully designed even in the millimeter-wave region. Fig. 14 shows the photographs of the external view of the filter and the fabricated windows with the surrounding metallic frame. Comparison between their calculated and measured frequency characteristics are given in Fig. 15. The measured results are limited in the frequency

Table 2. Dimension of the frequency selective windows in the millimeter-wave region.

	Window 1	Window 2	Window 3		Window 1	Window 2	Window 3
x_1	0.04 mm	0.05 mm	0.09 mm	y_4	0.06 mm	0.34 mm	0.47 mm
x_2	0.34 mm	0.40 mm	0.82 mm	y_5	0.10 mm	0.10 mm	0.07 mm
x_3	0.78 mm	0.89 mm	0.42 mm	y_6	0.24 mm	0.24 mm	0.22 mm
x_4	1.13 mm	0.46 mm	1.07 mm	g	0.11 mm	0.22 mm	0.27 mm
x_5	0.17 mm	0.24 mm	0.04 mm	d_1	1.41 mm	1.62 mm	2.03 mm
y_1	0.49 mm	0.06 mm	0.04 mm	d_2	1.47 mm	2.27 mm	2.31 mm
y_2	0.22 mm	0.19 mm	0.14 mm	l_1	1.16 mm	0.99 mm	0.84 mm
y_3	0.07 mm	0.15 mm	0.13 mm	l_2	1.21 mm	1.77 mm	1.19 mm

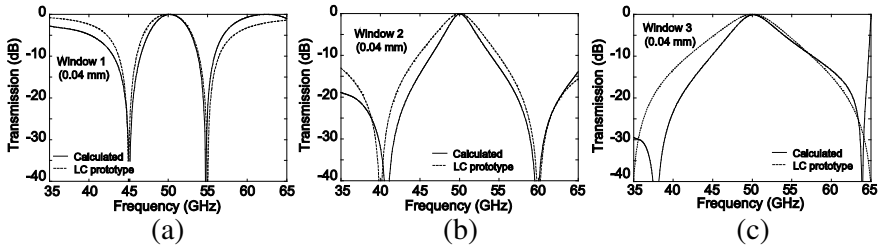


Figure 12. Comparison of transmission characteristic between the calculated results of the designed windows of 0.04 mm in thickness and the equivalent circuit approach. (a) Window 1, (b) window 2 and (c) window 3.

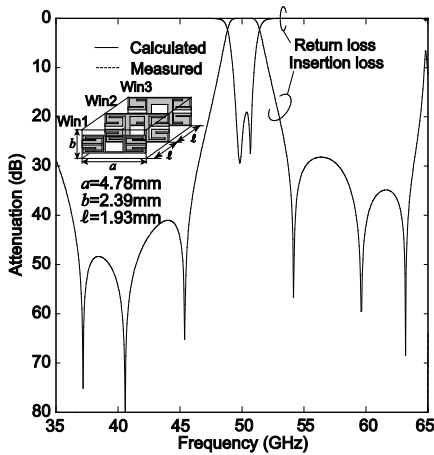


Figure 13. Calculated frequency characteristics of insertion and return losses for the designed filter in the millimeter-wave region.

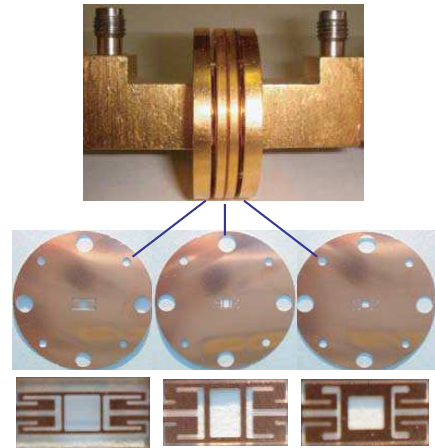


Figure 14. Photograph of the external view of the filter and three fabricated windows.

range from 40 GHz to 60 GHz. Fig. 16 shows the insertion and the return losses of the bandpass filter constructed by using three fabricated windows, where the dotted lines indicate the measured results and the solid lines are the calculated ones. In the calculation, the conductor loss ($\sigma = 5.8 \times 10^8 \text{ S/m}$) of the copper is taken into account. We can see a little deviation between both results. The precision of the size in the millimeter-wave filter requires the order of $10 \mu\text{m}$, but that of the filter fabricated in our laboratory is the order of $100 \mu\text{m}$. So the fabrication error causes the deviation between them.

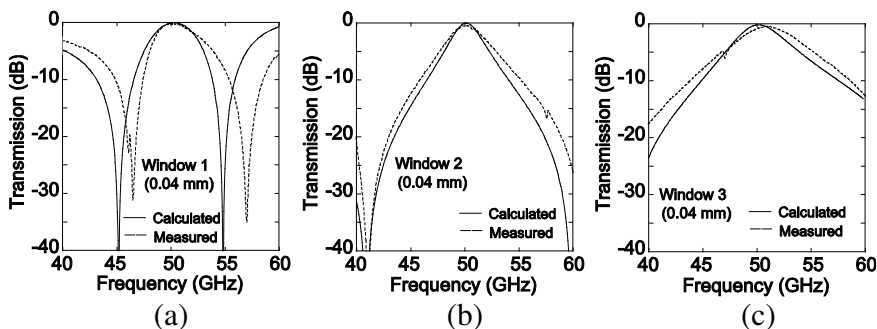


Figure 15. Comparison of transmission characteristic between the calculated results of the designed windows of 0.04 mm in thickness and the measured ones. (a) Window 1, (b) window 2 and (c) window 3.

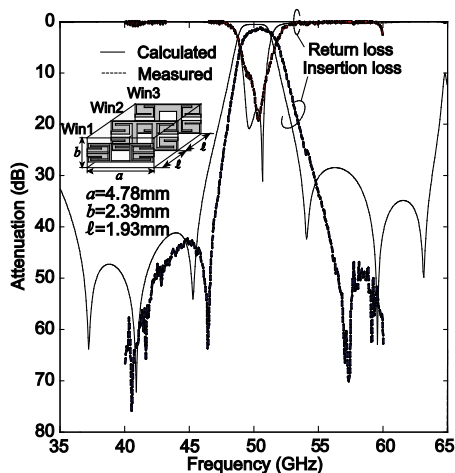


Figure 16. Comparison of insertion and return losses of the designed filter with the 0.04-mm-thick windows between the calculated and the measured results. In the calculation, the conductor loss ($\sigma = 5.8 \times 10^8 \text{ S/m}$) of the copper is taken into account.

5. CONCLUSION

This paper has proposed a new frequency selective window having a dual-behavior resonance, which is provided by utilizing the combination of the aperture-type and the patch-type resonances. As examples, 3-pole Chebyshev bandpass filters with six attenuation poles have been designed in the microwave and the millimeter-wave

regions. The filter can realize low insertion loss in a passband and the sharp cutoff skirt out of band without any additional coupling structures. The validity of the filter using the proposed frequency selective windows has been proven from good agreement of the filter characteristics between the measured and the calculated results in the microwave region. Then this design method has been applied in the millimeter-wave region, but a little deviation between both results has been observed, because it is difficult to make the fabrication error small in this region. We are now investigating to design the narrow-band filter.

ACKNOWLEDGMENT

This work was supported in part by a Grant-in-Aid for Scientific Research (C) (19560359) from Japan Society for the Promotion of Science.

REFERENCES

1. Shen, T. and K. A. Zaki, "Length reduction of evanescent-mode ridge waveguide bandpass filters," *Progress In Electromagnetics Research*, Vol. 40, 71–90, 2003.
2. Bahrami, H., M. Hakkak, and A. Pirhadi, "Analysis and design of highly compact bandpass waveguide filter using complementary split ring resonators (CSRR)," *Progress In Electromagnetics Research*, Vol. 80, 107–122, 2008.
3. Ghorbaninejad, H. and M. Khalaj-Amirhosseini, "Compact bandpass filters utilizing dielectric filled waveguides," *Progress In Electromagnetics Research B*, Vol. 7, 105–115, 2008.
4. Quendo, C., E. Rius, and C. Person, "Narrow bandpass filters using dual-behavior resonators," *IEEE Trans. Microwave Theory Tech.*, Vol. 51, No. 3, 734–743, Mar. 2003.
5. Quendo, C., E. Rius, and C. Person, "Narrow bandpass filters using dual-behavior resonators based on stepped impedance stubs and different-length stubs," *IEEE Trans. Microwave Theory Tech.*, Vol. 52, No. 3, 1034–1044, Mar. 2004.
6. Piloni, M., R. Ravenelli, and M. Guglielmi, "Resonant aperture filters in rectangular waveguide," *IEEE MTT-S Int. Microwave Symp. Dig.*, 911–914, Anaheim, CA, Jun. 1999.
7. Capurso, M., M. Piloni, and M. Guglielmi, "Resonant aperture filters: Improved out-of-band rejection and size reduction," *Proc.*

- of 31st European Microwave Conf.*, Vol. 1, 331–334, London, UK, Sep. 2001.
8. Ohira, M., H. Deguchi, M. Tsuji, and H. Shigesawa, “Novel waveguide filters with multiple attenuation poles using dual-behavior resonance of frequency-selective surfaces,” *IEEE Trans. Microwave Theory Tech.*, Vol. 53, No. 11, 3320–3326, Nov. 2005.
 9. Ohira, M., H. Deguchi, M. Tsuji, and H. Shigesawa, “Circuit synthesis for compact waveguide filters with closely-spaced frequency selective surfaces,” *10th Int. Symp. on Microwave and Optical Tech.*, 811–814, Fukuoka, Japan, Aug. 2005.
 10. Ohira, M., H. Deguchi, M. Tsuji, and H. Shigesawa, “A new dual-behavior FSS resonator for waveguide filter with multiple attenuation poles,” *Proc. of 35th European Microwave Conf.*, 189–192, Paris, France, Oct. 2005.
 11. Ohira, M., H. Deguchi, M. Tsuji, and H. Shigesawa, “A novel waveguide bandpass filter with multiple attenuation poles using four-armed square-loop FSSs,” *IEICE Trans. Electron. (Japanese Edition)*, Vol. 89, No. 7, 458–465, Jul. 2006.
 12. Seager, R. D., J. C. Vardaxoglou, and D. S. Lockyer, “Close coupled resonant aperture inserts for waveguide filtering applications,” *IEEE Microw. Wireless Comp. Lett.*, Vol. 11, No. 3, 112–114, Mar. 2001.
 13. Monorchio, A., G. Manara, U. Serra, G. Marola, and E. Pagana, “Design of waveguide filters by using genetically optimized frequency selective surface,” *IEEE Microw. Wireless Comp. Lett.*, Vol. 15, No. 6, 407–409, Jun. 2005.
 14. Ohira, M., H. Deguchi, and M. Tsuji, “A novel resonant window having dual-behavior resonance for pseudo-elliptic waveguide filter,” *Proc. of 36th European Microwave Conf.*, 1083–1086, Manchester, England, Sep. 2006.
 15. Matthaei, G. L., L. Young, and E. M. T. Jones, *Microwave Filters, Impedance-Matching Networks, and Coupling Structures*, McGraw-Hill, New York, 1964.